

Grand canonical validation of the bipartite International Trade Network

Mika J. Straka,¹ Guido Caldarelli,^{1,2,3} and Fabio Saracco¹

¹*IMT School for Advanced Studies, Piazza San Francesco 19, 55100 Lucca, Italy*

²*Istituto dei Sistemi Complessi, CNR, Dip. Fisica Università “Sapienza”, P.le A. Moro 2, 00185 Rome, Italy*

³*London Institute of Mathematical Sciences, 35a South St, Mayfair London W1K 2XF, UK*

Devising strategies for economic development in a globally competitive landscape requires a solid and unbiased understanding of countries’ technological advancement and similarities among export products. Both can be addressed through the bipartite representation of the International Trade Network. In the present paper, we apply the recently proposed grand canonical projection algorithm to uncover country and product communities. Contrary to past endeavors, our methodology, based on information theory, creates monopartite projections in an unbiased and analytically tractable way. Single links between countries or products represent statistically significant signals, which are not accounted for by null-models such as the Bipartite Configuration Model. We find stable country communities reflecting the socioeconomic distinction in developed, newly industrialized, and developing countries. Moreover, the product network exhibits a partition into clusters based on the aforementioned country groups.

INTRODUCTION

The application of the network formalism in the field of socioeconomic science has seen an unprecedented growth in the last decades [1–3]. Most of our actions take place in network environments and neglecting such structures can lead to insufficient interaction models [4, 5] and poor policy regulation [6].

On the global scale, the analysis of the International Trade Network (ITN), also known as World Trade Web, has taken a prominent role in the study of economic systems [7–10] motivated by the ongoing process of globalization. To assess the evolution of countries’ productive capabilities, international trade can be represented as a bipartite network between countries and products, which permits capturing the economic complexity of countries through the exclusiveness of their export baskets [11, 12]. At the same time, this approach offers the possibility to uncover relations among products. In fact, as countries can be divided according to their economic development, products can be clustered based on their exporters’ level of industrialization.

Several works [13–15] have proposed the derivation of a product network by projecting the ITN on the product layer. However, very often those methods are either too tailored to the problem and lack generalizability, or the definition of similarity between products neglects a comparison to the expectations of a statistical null-model. Although the last statement may appear to be an extraordinary strict request, it is crucial: a null-model permits to correctly discount important information and to distinguish between random fluctuations and statistically significant signals. Surprisingly few general methods for monopartite projections are present in literature, among which the seminal method proposed in [16] is worth mentioning. In the article, the authors

suggest a general framework to validate links statistically in the projected network. The original bipartite network is sliced into subsets that are homogeneous in the degree of nodes of one layer, which makes it possible to test analytically whether the observed co-occurrences are statistical significance, assuming that link distributions are uniform in each slice. Even though this approach is poorly effective due to the high number of hypotheses to be tested and the arguably unnatural slicing procedure, it establishes the right approach in terms of statistical verification.

Recently, great efforts have been spent in providing an unbiased monopartite projection for bipartite networks [17–19]. Summarizing, the method consists in comparing the total number of common neighbors of each couples of nodes belonging to the same layer to the expectation derived from the Bipartite Configuration Model (BiCM) [20]. Two nodes are subsequently linked in the projection if their number of common links in the original bipartite network is statistically significant. Although the framework originally uses the BiCM, which is the bipartite extensions of exponential random graph [20], it can be easily extended for other null-model. In fact, the BiCM may be too “strict” and account for all the observations in the data, and therefore cannot provide a projection of statistically significant co-occurrences of links. A related null-model is the partial BiCM (BiPCM) [19], which discounts less information than the original BiCM.

In the present paper, we apply the BiCM methodology mentioned above, referred to as the *grand canonical projection algorithm* whose features are explained in detail in [19], to the International Trade Network. This approach allows us to uncover stable country communities characterized by similar economic developments. At the same time, products cluster in groups which reflect the industrial advancements of their

exporters.

We observe that the BiCM induces a community structure which largely agrees with the socioeconomic distinction between developed, newly industrialized, developing and mainly raw material exporting countries. Interestingly, our analysis reveals a division within the group of developed countries around year 2000 into a core (Germany, USA, Japan, France, etc.) and a periphery (Austria, Italy, Spain, Eastern European countries, etc.), with the latter acting as a bridge to developing countries.

In addition, the formation of the product communities can be explained in terms of their exporters. For example, the presence of a highly technological chemistry cluster mirrors the exportation of such product by developed countries, whereas the focus of newly industrialized and developing countries on electronic devices, textiles and garments describes the appearance of such communities in the product network.

The paper is organized as follows. Firstly, we briefly introduce the ingredients of the grandcanonical projection algorithm in the Methods section. Details on the BiCM and related null-models can be found in the Appendix A and in the original article [19]. Secondly, the Results section presents the monopartite projections obtained from the null-models and illustrates the uncovered composition of country communities, which reflect their stages in economic development. Similarly, product communities are found based on their technological sophistication. Finally, we comment on the results and the performance of the methodology in the Conclusions.

METHODS

We consider a binary bipartite network composed of two distinct node sets and collection of undirected and unweighted edges. In the following, we will distinguish the nodes sets as N_i and N_α by using Latin and Greek indices, respectively, and will use the terms “sets” and “layers” interchangeably. The bipartite network can be described by a binary biadjacency matrix M of dimension $N_i \times N_\alpha$, where edges between node couples (i, α) are represented by the matrix entries $M_{i\alpha} = 1$.

It is intuitive that the bipartite network structure should contain information on the relationships of nodes in the same layer via their shared nearest neighbors. A common approach to access this information is to project the bipartite network on the layer of interest by considering only the respective nodes and linking them with edges whose weights are equal to the number of common neighbors in the original network. Even though this method is direct and intuitive, it neglects the crucial problem of determining which edges contain statistically

relevant information and which do not.

To address this question, in the present paper we employ the grand canonical projection methodology proposed in [19], since it provides exact results and a coherent formalism. In the following, we will briefly review the method, inviting the interested reader to the original article.

Grand canonical projection

The grand canonical projection algorithm proposed in [19] yields a statistically validated monopartite projection of a bipartite network by comparing the observed node similarities with the expectations from a suitable null-model.

Bipartite motifs as a measure of similarity The number of common neighbors shared by two nodes of the same Latin (Greek) layer can be used as a measure of similarity. It can either be expressed as the number of $K_{2,1}$ ($K_{1,2}$) bi-cliques [21] or, following the formalism of [20], as the number of V-motifs (Λ -motifs). As illustrated

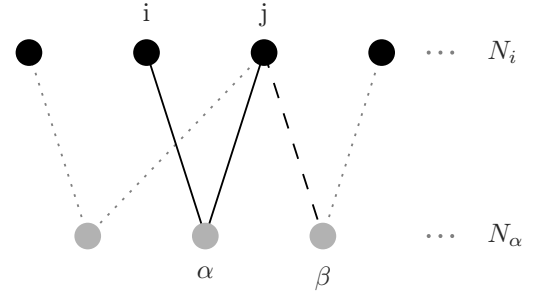


Figure 1: The V_α^{ij} -motif is illustrated by the bold black edges between node couples (i, α) and (j, α) .

Analogously, the edges between (j, α) and (j, β) describe the $\Lambda_{\alpha\beta}^j$ -motif. The top layer contains the “Latin” nodes, the bottom the “Greek” nodes. Other edges are indicated by dotted gray lines.

in Fig.1, the number of V-motifs between node i and j , for instance, can be easily obtained from the biadjacency matrix as

$$V^{ij} = \sum_{\alpha} V_{\alpha}^{ij} = \sum_{\alpha} M_{i\alpha} M_{j\alpha}. \quad (1)$$

Bipartite Configuration Model and Bipartite Partial Configuration Models In order to establish whether two nodes are similar in a statistical sense, we compare the motif measurements with the expectations from the Bipartite Configuration Model (BiCM), as defined in [20]. The BiCM is a null-model which is based on the entropy

maximization principle while discounting the information on the degrees of all nodes on both layers. The philosophy behind its construction is similar to the Erdős Renyi Random Graph [22], though here the degree sequences of both layers are constrained rather than the total number of links (more details about the BiCM can be found in the Appendix). One of the powerful properties of the BiCM is that it provides independent link probabilities and is analytically tractable. Consequently, we can readily calculate the expectation values of several network observables. For instance, the average number of V -motifs between i and j is

$$\langle V^{ij} \rangle^{\text{BiCM}} = \sum_{\alpha} p_{i\alpha}^{\text{BiCM}} p_{j\alpha}^{\text{BiCM}}, \quad (2)$$

where $p_{i\alpha}^{\text{BiCM}}$ is the probability of observing a link between nodes i and α according to the BiCM. It is worth noting that the constraints, which are imposed in the creation of a null-model, specify which network quantities should be accounted for in the statistical validation process. As a consequence, it may happen that the constraints turn out to be too strict, meaning that they capture the main information contained in the network and thus attribute high probabilities to the actually observed V -motif values. In our case, one can relax the constraints on the degree sequence in the BiCM and only fix the degrees of a single layer. This model has been proposed as Bipartite Partial Configuration Model (BiPCM, [19]) and will also be applied in the following.

Statistical Significance of Node Similarities: p -Values and False Discovery Rate Both null-models, BiCM as well as BiPCM, provide closed forms for the probability distributions of the Λ - and V -motifs. In the case of the BiCM, they follow a generalization of the binomial distribution, called Poisson-Binomial distribution [23–25], for every node couple. At the same time, the BiPCM behaves quite differently depending on the layer whose degrees are constrained. As mentioned in [19], the model performs well if the degrees of the projection layer are constrained in the null-model, which is not the case if the degrees of the opposite layer are fixed. In fact, the latter amounts to ignore the heterogeneity of the degrees of the projection layer, leading to the same theoretical distribution for each node couple, while, in the former case the probability distributions are distinct for each node couple. The effective limits of the partial configuration models are currently under investigation. By comparing the observed bipartite motifs with their expectations from the null-model it is possible to calculate the p -values, i.e. the cumulative probability of observing a value greater or equal to the actual measurement. In a nutshell, a p -value smaller than a predefined threshold implies that the observed number is not explainable by the information contained in the null-model. In this sense, the smaller the p -value, the larger the similarity between the respective nodes, compared with

the null-model expectation. It is customary, in this case, to control the False Discovery Rate (FDR) [26], which is, in fact, the only method for multiple hypotheses testing which has a strict control on every step of the validation. Once the p -values are validated, the projection network can be obtained by connecting only the nodes which share a statistically significant link. In the following, the significance level of all validated networks is $\alpha = 0.01$.

An open-source implementation in Python of the null-models and the calculation of the p -values is available on the web [27]. More details on the bipartite configuration models, the similarity measures and their distributions can be found in the Appendix.

DATA

In the present paper, we focus on the information contained in the global product exportation. The ITN is thus represented as a bipartite network composed of a product and a country layer. An edge between two nodes α and i symbolizes the exportation of product α by country i . We use the BACI HS 2007 database from CEPII [28] to construct the bipartite network, which comprises the export data for the years 1995 - 2010. Products are identified according to the Harmonized System and organized in hierarchical categories at different aggregation levels, which are captured by two, four, or six digit product codes. Here, we adopt the 2007 code revision (HS 2007) with four digit codes for 1131 different products. The BiCM and BiPCM can be applied to binary networks, which necessitates the conversion of export values from US\$ into a binary form. For this purpose, we apply the concept of revealed comparative advantage (RCA), also referred to as Balassa index [29]. It describes whether a specific country is a relevant exporter of a product ($RCA \geq 1$) or not ($RCA < 1$) by comparing the relative monetary importance of the product in the country's export basket to the global average. The RCA is defined as

$$RCA_{c,p} = \frac{e(c,p)}{\sum_{p'} e(c,p')} \bigg/ \frac{\sum_{c'} e(c',p)}{\sum_{c',p'} e(c',p')}, \quad (3)$$

where $e(c,p)$ denotes the export value of product p in country c 's export basket.

Basic properties on the binary biadjacency matrix of ITN

In the bipartite ITN, the degree distributions resemble a power-law for the countries and a Gaussian for the products. The degree heterogeneity can be approximately captured by the coefficient of variation (CV), i.e. the standard deviation over the mean, $\frac{\sigma}{\mu}$. As a rule of thumb, the

larger the CV the less informative is the mean about the whole distribution. In the present data set, the CV varies between 0.5 and 0.55 for the products and between 0.82 and 0.89 for the countries. As a consequence, neglecting the degree distribution of the countries incurs a comparatively bigger loss of information than it would be the case for the products.

In the data set we examine, the number of products is almost 10 times the number of countries and the bi-adjacency matrix hence strongly rectangular. The connectance varies during the years between 0.09 and almost 0.13. This feature is probably related to the division of products in categories (see [30]).

RESULTS

Country layer projection

The projection on the country layer induced by the BiCM reveals important information on different levels of economic development and the roles played by various countries in the globalization process.

Applying an enhanced version of the Louvain community detection [31] throughout the years, four stable communities can be observed, as depicted in Fig. 2: developed countries (in blue), centered around Germany, USA, Japan, UK, and other European countries; newly industrialized and developing countries (in purple), comprehending China, India, Turkey, Southeast Asia, and some Central American countries; developing countries in Africa and South America (in green); developing countries exporting mainly raw materials such as oil (in orange), encompassing Russia, Saudi Arabia, Venezuela, post-Soviet states and North African countries. Furthermore, one can discern a fifth group whose composition fluctuates strongly during the considered time interval. It is mainly composed of countries which large coastal regions, who have little access to neighboring countries via continental trade routes. The community includes, among others, Australia, New Zealand, Canada, Chile, and Argentina. Much of their industrial output is aimed at internal markets and exports are strong in the fishing sector, especially for Canada and Chile. This explains why they are loosely linked to poorly industrialized nations like Mauritania, whose most important trade goods derive from fishing activities. As a result of the weak connectivity within the group, countries oscillate between different communities, which can clearly be seen, for example, for Australia and Canada in Fig. 2.

Relaxing the conditions of the null-model to the degree sequence of the country layer leads to a BiPCM_c-induced projection. The community structure is more stable than for the BiCM. In particular, note in Fig. 4 that the fluctuating community disappears and that

the division of countries seems more static. Weakening the constraints of the null-model smooths out the noise in the projection. As a matter of fact, neglecting the constraints on the product layer means losing the information on the product degree distribution by substituting it with a Delta distribution at the average degree. Thus, the approximation is more accurate the smaller the relative dispersion of the product degrees, which is captured by the coefficient of variation and amount to around 0.5 in our case (see “Data” section).

The downside of the stability of the BiPCM_c projection is that the smoothing covers small but insightful structural changes. For instance, the BiCM manages to capture the separation of the developed European countries in an Eastern and a Western part during the

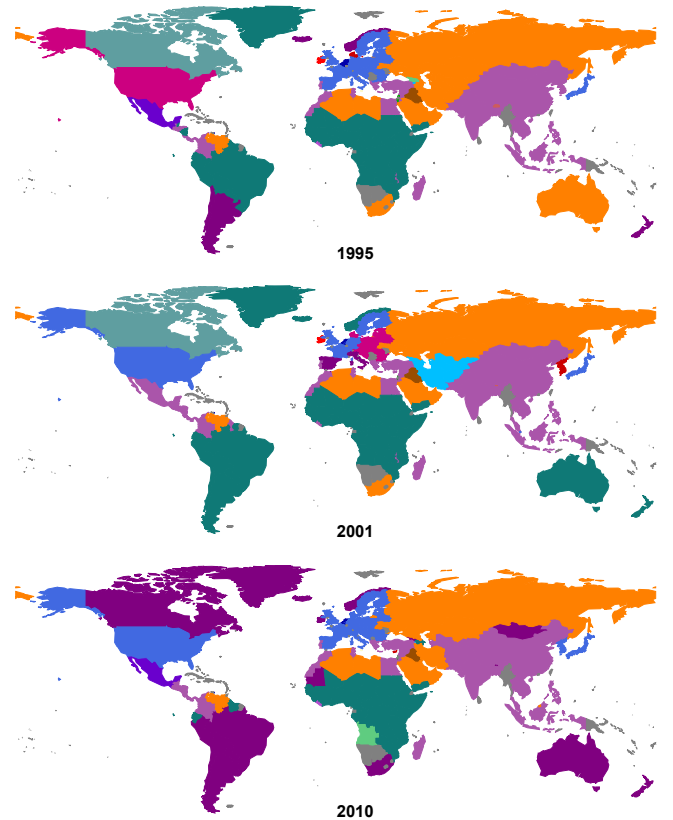


Figure 2: Communities of countries based on BiCM projection for the years: 1995, 2001, 2010. Even though the communities show some noise, the partition in the following communities is stable: developed countries (blue), newly industrialized and developing countries (light purple), developing countries (green), and countries relying their export on raw materials, e.g. oil (orange).

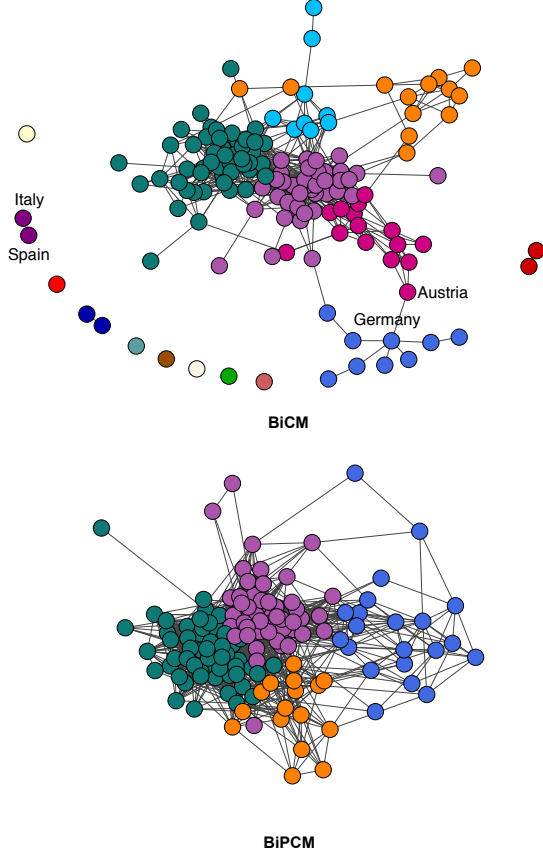


Figure 3: Structure of the projected country network obtained with the BiCM and the BiPCM for the year 2001. Note that in weakening the constraints, i.e. passing from BiCM to BiPCM, the connectance increases.

years 1997-2002 and the split-off of Italy and Spain, see Fig. 3. Interestingly, Germany and Austria form a bridge between the Western and Eastern nations, with the latter themselves connecting to developing countries.

Another striking result of the analysis of the country projection is the fact that many post-Soviet states still share a similar economic development years after the dissolution of the Soviet Union. A similar signal was detected in [32].

Product layer projection

The BiCM-induced projection of the bipartite ITN network on the product layer does not reveal any statistically significant relations, as already mentioned in [19, 33]. In other words, the degree sequence of both countries and products contains enough information to account for the observed product similarities in terms of

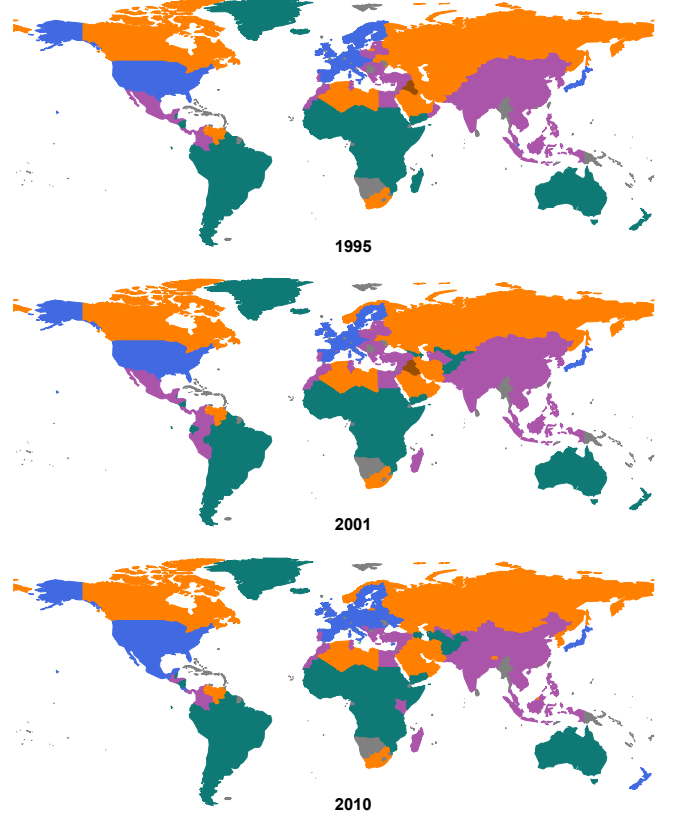


Figure 4: Country communities based on the BiPCM_c projection for the years: 1995, 2001, 2010. Compared to the BiCM communities of Fig. 2, the partition here is more stable.

the Λ -motifs.

This observation stands in stark contrast to the country projection and is mainly due to two reasons connected to the different cardinalities of the layers. Firstly, the effective p -value threshold for the validation procedure is proportional to the ratio of the significance level α over the number of tests, i.e. $\propto \alpha / \binom{N}{2}$ for N nodes as shown in Appendix A. Hence, the statistical validation is more restrictive on “longer” layers. In our case, the product layer is almost ten times larger than the country layer, which leads to a comparatively smaller effective threshold level. Secondly, the variability of node degrees in a layer depends on the length of the opposite layer, since each node can have a degree between one and the total number of elements in the latter if it is fully connected. The degree heterogeneity of the longer layer is thus generally more limited compared to the shorter layer, which reduces the possible different values of the bipartite motifs between products, in our case.

Due to the behaviour of the BiCM, we used the

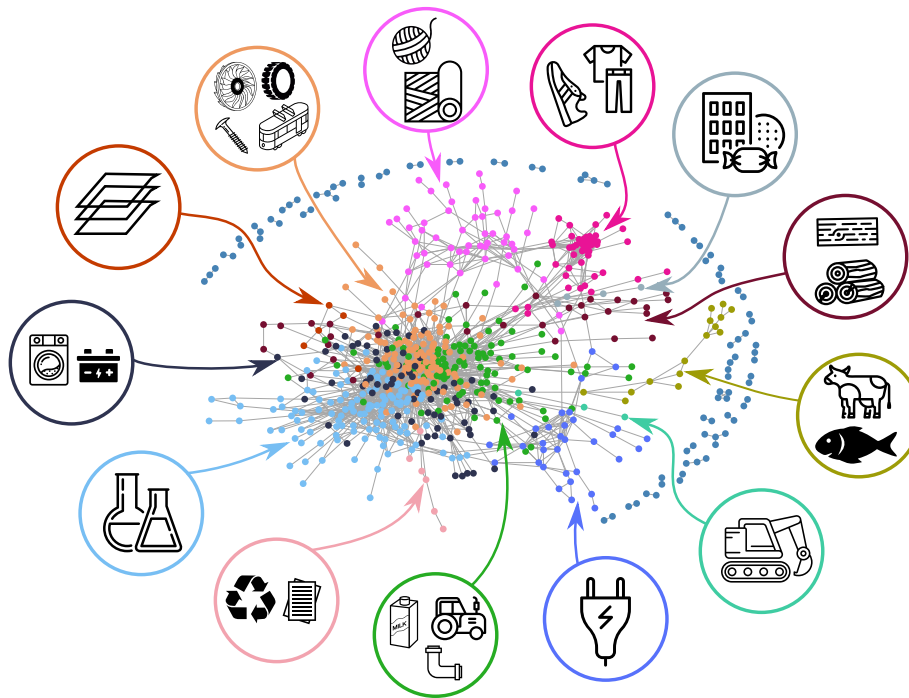


Figure 5: BiPCM_p product network spanned by FDR validated edges for $\alpha = 10^{-2}$ in the year 2000. The communities have been obtained using the Louvain algorithm and include: ● fabrics, yarn, etc.; ● clothes, shoes, etc.; ● wooden products; ● animal products; ● basic electronics; ● chemicals; ● machinery; ● advanced electronics and machinery (Icons designed by the authors and Freepik, Madebyoliver, and Eucalyp from Flaticon).

BiPCM_p, i.e. the configuration model in which only the product degrees are constrained, to perform the validation procedure for product similarities. As mentioned in the “Methods” section, constraining the degrees of the projected layer is more effective because the resulting probability distribution of the V -motifs resembles more the BiCM distribution [19]. However, since the degree sequence of the countries, whose observed CV is almost $\simeq 0.8$, is approximated by a Delta distribution in this approach, we have to take a loss of information into account. The product co-occurrences are thus observed discounting only the degree sequence of the products in the null-model.

The BiPCM_p-induced product networks are sparse with connectances in the range of 0.009-0.013 and highly fragmented for the years 1995-2010. As shown by the Jaccard indices of the edge sets in Fig. 6, they are quite dissimilar from year to year. In the country networks on the contrary, the value never falls below 0.75 and 0.8 for the BiCM and BiPCM_c, respectively. Nevertheless, the signal of product similarity persists: in fact, the shuffled Louvain community detection algorithm discovers a community structure that is stable throughout the years. The projection pinpoints evidently close relationships and captures broader communities of high technology

chemicals, electronic devices, garments and textiles, etc. The communities remain constant, although the single links do not.

Going into detail, the BiPCM_p network consists of many small clusters surrounding a central largest connected component (LCC), see Fig. 5 for the year 2000. Most of the isolated clusters are composed of vegetables, fruits, and their derivatives, such as lettuce and cabbage, soybeans and soybean oil, or fruit juice and jams. Other connections are less trivial: lead ores and zinc ores, for instance, are typically present in the same geological rock formations and appear as an isolated component in the network [33].

The application of the shuffled Louvain community detection algorithm uncovers a rich community structure inside the LCC, as shown in Fig. 5 for the year 2000. In the outer regions of the LCC we observe well-defined clusters, the most prominent of them being the garment and textile cluster containing clothes and shoe products. Furthermore, one can discern a distinct community containing electrical equipment, such as circuits, diodes, telephones, and electrical instruments. Other clusters comprise bovine and fish products, yarns and fabrics, and goods made out of wood, such as planks, tool handles, etc.

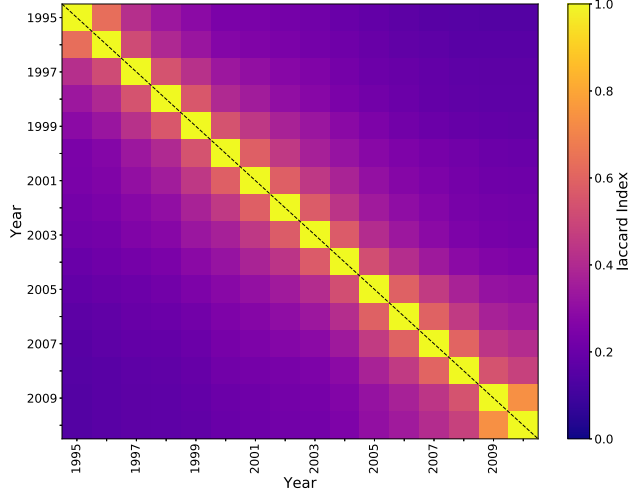
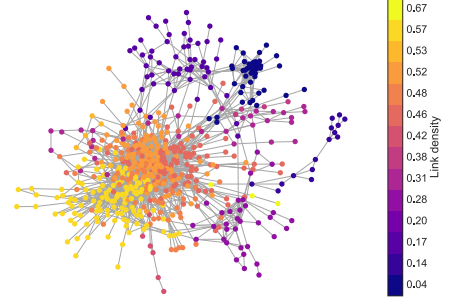


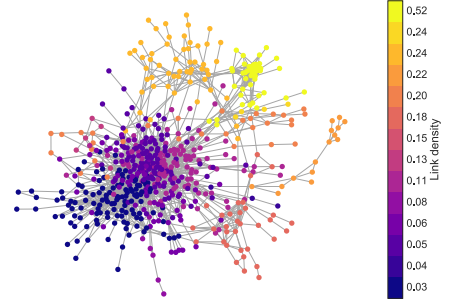
Figure 6: Comparison of the product networks for the years 1995-2010. The Jaccard index measures the similarity between their edge sets, E and is defined as $|E_{year_i} \cap E_{year_j}| / |E_{year_i} \cup E_{year_j}|$. The values fall very quickly below 0.5 for $|year_i - year_j| > 2$.

The core of the LCC, on the other hand, hosts several overlapping communities containing mostly more sophisticated products, such as motors and generators, machines, cars, turbines, arms, chemical products, antibiotics, and other industrial products. The community compositions are subject to fluctuations and include also, for example, agriculture and dairy products. The fuzziness of the core communities is due to the fact that they are typically exported by “developed” countries, which have large exportation baskets [11, 12, 34, 35].

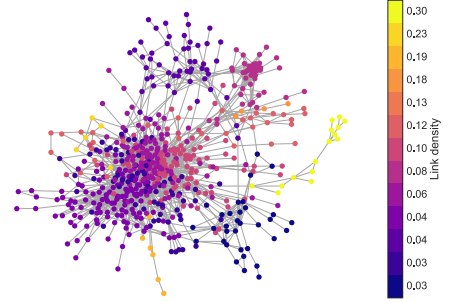
Note that the product communities do not follow necessarily the HS 2007 categorization, which is evident for the core communities where commodities of different origins can be found. As depicted in Fig. 5, the green community, for example, comprises milk, heavy-duty vehicles, and pipes. Although this may seem confusing at first sight, it is largely due to the fact that the projection derives originally from the exportation network and should reflect the different levels of industrialization of the exporting countries. This behavior is shown in Fig. 7: different country communities occupy mostly different product communities, as is captured by the index $ICP = \frac{\sum_{i \in C, \alpha \in P} M_{i\alpha}}{|C||P|}$, i.e. the density of links between country community C and product community P [19]. Developed countries focus on the core communities and export, for instance, high technological machinery and sophisticated chemical products. At the same time, however, their export baskets encompass also products



(a) Developed countries



(b) Newly industrialized & developing countries



(c) Raw material exporters

Figure 7: The images show the relative focus of the country communities' exportation on different product cluster of the BiPCM_p product network for the year 2000: (a) developed countries occupy the central communities of high technological and chemical products; (b) developing countries focus on peripheral communities with relatively low complexity [34, 35]; (c) raw material exporters are comparatively less focused, as shown in the link densities.

of low complexity such as milk and pipe, which are also exported, in fact, by newly industrialized countries next

to textile products, garments, etc. In other words, the communities we observe, both on the product and the country layer, are derived from the way items interact: similar exports define countries with similar industrial development and, on the other hand, similar exporters define products with the same technological level.

CONCLUSIONS

The representation of international trade as a bipartite network between countries and their exportation provides the perfect framework to assess the question of economic development and to analyze the relation between products [11–14, 34, 35]. Accomplishing these tasks should advisably take the complete network and not only the single export baskets into account [34, 35]. A suitable strategy is to perform an unbiased monopartite projection of the bipartite network, as recently proposed in the literature [17–19]. Such an approach is based on the whole information contained in the network structure. In particular, the Bipartite Configuration Model (BiCM) provides a relevant benchmark, being an unbiased and analytically tractable null-model rooted in the principle of entropy maximization [20]. It discounts the information contained in the degree sequence of the network and allows us to assess the statistical significance of node similarity through the grand canonical projection algorithm [19]. Generally speaking, this method leaves room for the definition of other opportune null-models by modifying the topological constraints. In fact, restraining the whole degree sequence can turn out to be too strict and may suggest relaxing the constraints to only one bipartite layer, yielding the partial BiCM (BiPCM). Not surprisingly, the BiPCM works best if the degrees of those nodes are fixed the network is projected on, since this information is more relevant for establishing similarities between them [19].

In the present paper, we built on [19] and applied the methodology illustrated above to the International Trade Network of Economic Complexity in order to uncover relation among countries and among products. Some proposals have been presented in the literature [13–15], but none of them implemented well established first principles methods.

The application of the BiCM to the ITN as a statistical null-model permits to uncover communities of countries with similar economic development, namely developed, newly industrialized, and developing countries, and raw material (e.g. oil) exporters. These groups are stable during the considered years 1995–2010 except for some small deviations due to, for instance, different progress in the ongoing globalization process. The communities become even more stable using the BiPCM

for the monopartite projection. At the same time, however, the BiPCM is not able to detect smaller details like, for example, the post-Soviet state community. Regarding the product layer, the BiCM turns out to be too restrictive to uncover any significant product similarities. In other words, the information contained in the degree sequence of both layers is enough to account for the observed product relations in the data. This limitation is due to the “rectangularity” of the network, i.e. the ratio of the two bipartite layer lengths. As a matter of fact, this behavior has not been observed before and necessitates a relaxation of the constraints in order to investigate the similarity among products, logically leading to the application of the BiPCM. Using the BiPCM, we find product communities which define different industrialization levels and reflect the economic stages of their exporting countries. Highly sophisticated chemical products distinguish developed from newly industrialized and developing countries, whose exports focus mainly on electronic articles like diodes and telephones, or textiles and garments. It is worth pointing out that the communities are generally not due to productive chains, which should be reflected in a tree-like organization of the network. This observation suggests that they are rather defined by the way countries organize their export baskets.

In sum, the grandcanonical projection algorithm marks an important step in the research on bipartite networks and could be extended to directed or weighted networks in future endeavors. Moreover, solid criteria for the choice of the null-model are still absent and leave room for improvement.

ACKNOWLEDGMENTS

This work was supported by the EU projects CoeGSS (grant num. 676547), Multiplex (grant num. 317532), Shakermaker (grant num. 687941), SoBigData (grant num. 654024) and the FET projects SIMPOL (grant num. 610704), DOLFINS (grant num. 640772). The authors acknowledge Giulio Cimini, Riccardo Di Clemente, Luca Pappalardo, Tiziano Squartini and all participants to NEDO Journal Club for useful discussions.

-
- [1] A. L. Barabási, *Nature Physics* **8**, 14 (2011).
 - [2] G. Caldarelli, *Scale-Free Networks: Complex Webs in Nature and Technology* (Oxford University Press, Oxford (UK), 2010) pp. 1–328.
 - [3] R. Pastor-Satorras and A. Vespignani, *Nature Physics* **6**, 480 (2010).
 - [4] M. Catanzaro and M. Buchanan, *Nature Physics* **9**, 121 (2013).

- [5] M. O. Jackson, *The Journal of Economic Perspectives* **28**, 3 (2014).
- [6] S. Battiston, J. D. Farmer, A. Flache, D. Garlaschelli, A. G. Haldane, H. Heesterbeek, C. Hommes, C. Jaeger, R. May, and M. Scheffer, *Science (New York, N.Y.)* **351**, 818 (2016).
- [7] M. A. Serrano and M. Boguñá, *Physical review. E, Statistical, nonlinear, and soft matter physics* **68**, 015101 (2003).
- [8] K. Bhattacharya, G. Mukherjee, J. Saramäki, K. Kaski, and S. S. Manna, *Journal of Statistical Mechanics: Theory and Experiment* **2008**, P02002 (2008), [arXiv:0707.4343](https://arxiv.org/abs/0707.4343).
- [9] M. Barigozzi, G. Fagiolo, and D. Garlaschelli, *Physical Review E* **81**, 046104 (2010).
- [10] R. Mastrandrea, T. Squartini, G. Fagiolo, and D. Garlaschelli, *Physical Review E - Statistical, Nonlinear, and Soft Matter Physics* **90** (2014), 10.1103/PhysRevE.90.062804, [arXiv:arXiv:1307.2104v2](https://arxiv.org/abs/1307.2104v2).
- [11] C. A. Hidalgo and R. Hausmann, *Proceedings of the National Academy of Sciences of the United States of America* **106**, 10570 (2009).
- [12] R. Hausmann and C. A. Hidalgo, *Journal of Economic Growth* **16**, 309 (2011).
- [13] C. A. Hidalgo, B. Klinger, A.-L. Barabasi, and R. Hausmann, *Science* **317**, 482 (2007).
- [14] G. Caldarelli, M. Cristelli, A. Gabrielli, L. Pietronero, A. Scala, and A. Tacchella, *PLoS ONE* **7**, 1 (2012), [arXiv:1108.2590](https://arxiv.org/abs/1108.2590).
- [15] A. Zaccaria, M. Cristelli, A. Tacchella, and L. Pietronero, *PLoS ONE* **9**, 1 (2014), [arXiv:1408.2138](https://arxiv.org/abs/1408.2138).
- [16] M. Tumminello, S. Miccichè, F. Lillo, J. Piilo, and R. N. Mantegna, *PLoS ONE* **6** (2011), 10.1371/journal.pone.0017994, [arXiv:1008.1414](https://arxiv.org/abs/1008.1414).
- [17] S. Gualdi, G. Cimini, K. Primicerio, R. Di Clemente, and D. Challet, *PLoS ONE* **11**, 1 (2016), [arXiv:1603.05914](https://arxiv.org/abs/1603.05914).
- [18] N. Dianati, (2016), [arXiv:1607.01735](https://arxiv.org/abs/1607.01735).
- [19] F. Saracco, M. J. Straka, R. Di Clemente, A. Gabrielli, G. Caldarelli, and T. Squartini, (2016), [arXiv:1607.02481](https://arxiv.org/abs/1607.02481).
- [20] F. Saracco, R. Di Clemente, A. Gabrielli, and T. Squartini, *Scientific reports* **5**, 10595 (2015).
- [21] R. Diestel, *Graduate Texts in Mathematics* (2010) pp. XVIII, 410, [arXiv:arXiv:1102.1087v6](https://arxiv.org/abs/1102.1087v6).
- [22] P. Erdos and A. Rényi, *Publicationes Mathematicae Debrecen* **6**, 290 (1959).
- [23] P. Deheuvels, M. L. Puri, and S. S. Ralescu, *Journal of Multivariate Analysis* **28**, 282 (1989).
- [24] A. Y. Volkova, *Theory of Probability & Its Applications* **40**, 791 (1996).
- [25] Y. Hong, *Computational Statistics and Data Analysis* **59**, 41 (2013).
- [26] Y. Benjamini and Y. Hochberg, *Journal of the Royal Statistical Society B* **57**, 289 (1995), [arXiv:95/57289](https://arxiv.org/abs/95/57289) [0035-9246].
- [27] <https://github.com/tsakim/bicm>, <https://github.com/tsakim/bipcm>.
- [28] <http://www.cepii.fr/>.
- [29] B. Balassa, *Manchester School* **33**, 99 (1965).
- [30] F. Saracco, R. Di Clemente, A. Gabrielli, and L. Pietronero, *PLoS ONE* **10** (2015).
- [31] Since the Louvain algorithm depends on the order in which nodes are considered [36], we made use of a more effective version of the original method. The community

detection is repeated for several iterations with shuffled node sequence and the community partition giving rise to the highest modularity is eventually kept. The Python code can be found at https://github.com/tsakim/Shuffled_Louvain.

- [32] F. Saracco, R. Di Clemente, A. Gabrielli, and T. Squartini, *Scientific Reports* **6**, 30286 (2016), [arXiv:1508.03533](https://arxiv.org/abs/1508.03533).
- [33] M. J. Straka, F. Saracco, and G. Caldarelli, *Complex Networks 2016 - Book of Abstracts*, 130 (2016).
- [34] A. Tacchella, M. Cristelli, G. Caldarelli, A. Gabrielli, and L. Pietronero, *Scientific Reports* **2**, 1 (2012).
- [35] M. Cristelli, A. Gabrielli, A. Tacchella, G. Caldarelli, and L. Pietronero, *PLoS ONE* **8** (2013).
- [36] S. Fortunato, *Physics Reports* **486**, 75 (2010), [arXiv:0908.1062](https://arxiv.org/abs/0908.1062).
- [37] J. Park and M. E. J. Newman, *Physical Review E* **70**, 066117 (2004).

APPENDIX A: GRAND CANONICAL NULL-MODELS AND NODE SIMILARITY

In the present appendix we revise briefly the methods of [19, 20], making use of the formalism introduced in the section “Methods”.

Bipartite Null-Models All configuration models of [19, 20] are based on the statistical mechanics approach to complex networks [37] and the Shannon entropy per graph defined as

$$S = - \sum_{G_B \in \mathcal{G}_B} P(G_B) \ln P(G_B). \quad (4)$$

Here, \mathcal{G}_B denotes an ensemble of bipartite graphs in which the number of nodes is constant, while the number of links is left able to vary; P is the probability of the bipartite graph G_B belonging to ensemble \mathcal{G}_B . The entropy (4) can be maximized subjected to the vector of constraints $\vec{C}(G_B)$. Solving the entropy maximization in terms of the probability per graph returns

$$P(G_B|\vec{\theta}) = \frac{e^{-\mathcal{H}(\vec{C}(G_B), \vec{\theta})}}{Z(\vec{\theta})}, \quad (5)$$

where $\mathcal{H}(\vec{C}(G_B), \vec{\theta})$ is the Hamiltonian of the system, encoding the constraints. $Z(\vec{\theta}) = \sum_{G_B \in \mathcal{G}_B} e^{-\mathcal{H}(\vec{C}(G_B), \vec{\theta})}$ the partition function and $\vec{\theta}$ is the vector of Lagrangian multipliers associated to the entropy maximization. Different types of null-models can be obtained by modifying the constraints in the Hamiltonian. For instance, by fixing the total number of edges $C = \sum_{i,\alpha} M_{i\alpha} = E$, we obtain the *Bipartite Random Graph* (BiRG), a bipartite version of the well-known Erdős-Rényi model [22]. In accordance with the constraints, its Hamiltonian is given by

$$\mathcal{H}_{BiRG} = \theta \cdot E. \quad (6)$$

In this case both \vec{C} and $\vec{\theta}$ are scalars, since there is just one condition. In the BiRG model, all edges are equally probable, with probability

$$p_{i\alpha}^{\text{BiRG}} = \frac{e^{-\theta}}{1 + e^{-\theta}} \quad \forall i, \alpha. \quad (7)$$

In the so-called *Bipartite Configuration Model* (BiCM) [20], the degrees of the nodes in both layers are fixed and the graphs of the ensemble are constructed accordingly. If k_i and k_α are the degrees respectively for the node i in the Latin layer and for the node α in the Greek layer and θ_i and θ_α the relative Lagrangian multipliers, the Hamiltonian reads thus

$$\mathcal{H}_{\text{BiCM}} = \sum_i \theta_i k_i + \sum_\alpha \theta_\alpha k_\alpha, \quad (8)$$

such that the probability is

$$p_{i\alpha}^{\text{BiCM}} = \frac{e^{-(\theta_i + \theta_\alpha)}}{1 + e^{-(\theta_i + \theta_\alpha)}}. \quad (9)$$

Relaxing the constraints of the BiCM yields the partial Bipartite Configuration Models, BiPCMs, introduced in [19]. In particular, we constrain only the degrees of nodes in one layer. The corresponding Hamiltonians read

$$p_{i\alpha}^{\text{BiPCM}_i} = \frac{e^{-\theta_i}}{1 + e^{-\theta_i}} \quad \forall \alpha \quad (10)$$

$$p_{i\alpha}^{\text{BiPCM}_\alpha} = \frac{e^{-\theta_\alpha}}{1 + e^{-\theta_\alpha}} \quad \forall i. \quad (11)$$

It is worth pointing out that the Hamiltonians for the null-models defined above are all linear in the constraints. In fact the linearity of the constraints permits to express the graph probability $P(G_B)$ in terms of the single link probabilities, i.e. as

$$P(G_B) = \prod_{i,\alpha}^{N_i, N_\alpha} p_{i\alpha}^{m_{i\alpha}} (1 - p_{i\alpha})^{1 - m_{i\alpha}}, \quad (12)$$

for any one of the null-model considered in the present section.

Node Similarity In [19] the similarity measure implemented is just the number of bi-cliques $K_{2,1}$ or $K_{1,2}$ [21] (or V- and Λ -motifs, using the terminology of [20]) existing between two nodes of the same layer. For instance, the number of all V-motifs between i and j , V^{ij} , in the binary bipartite network is therefore given by

$$V^{ij} = \sum_{\alpha \in N_\alpha} M_{i\alpha} M_{j\alpha} \quad (13)$$

The “standard” approach is to consider the V-motifs as the quantity to analyse; in the approach of [19], the statistical significance of every V^{ij} is stated with reference

to the aforementioned null-models in order to discount insignificant fluctuations and reveal relevant node similarities. The monopartite projection includes thus only edges (i, j) whose relative V^{ij} are statistically significant. Since edges are independent (see (12)), the probability of measuring a V-motif consisting of (i, j) on the Latin layer and α on the Greek layer is

$$P(V_\alpha^{ij}) = p_{i\alpha} p_{j\alpha}. \quad (14)$$

In the case of the Random Graph model, for instance, $P(V_\alpha^{ij})_{\text{BiRG}} \equiv (p^{\text{BiRG}})^2 \forall i, j \in N_i, \forall \alpha \in N_\alpha$, since the edge probability is independent of the couple (i, α) and uniform in the network. In this sense, the probability distribution of $V^{ij} = \sum_\alpha V_\alpha^{ij}$ is the sum of independent Bernoulli events, all with the same probability $(p^{\text{BiRG}})^2$, i.e. a Binomial distribution. In the Configuration Model, on the other hand, $p_{i\alpha}$ differs from couple to couple; V^{ij} is thus the sum of independent Bernoulli random variables, in general with different success probabilities. The probability of observing $P(V^{ij} = k)$ will therefore be given by

$$P(V^{ij} = k) = \sum_{\tilde{\alpha}_k \in A_k} \prod_{\alpha \in \tilde{\alpha}_k} P(V_\alpha^{ij}) \prod_{\alpha' \notin \tilde{\alpha}_k} (1 - P(V_{\alpha'}^{ij})) \quad (15)$$

where A_k is the set of all possible choices of k elements from the set $\{1, 2, \dots, N_\alpha\}$ and $\tilde{\alpha}_k$ is a single realisation, [25].

The Partial Configuration Models are a midway between the BiCM and BiRG: the distribution for V^{ij} is the same Poisson Binomial for all couples (i, j) in the case of BiPCM_α , while it is a Binomial distribution with probability $p = \frac{k^i k^j}{N_\alpha^2}$ for BiPCM_i . In fact, in reconstructing the structure of the V-motifs network it is much more effective to know the degrees of the nodes involved in the V-motifs than the nodes on the other layer, such that the BiPCM_i resulted as more accurate in the network reconstruction. The limits of this intuition are currently under analysis.

Statistical Hypothesis Testing and FDR Validating the statistical significance of the measured V^{ij} therefore revolves around the null hypothesis that its observed value can be explained by the underlying null-model, i.e. that it is compatible with the corresponding probability distribution. For this purpose, we calculate the p -values for right-tailed tests, i.e. $P(V^{ij} \geq V^{*ij})$, where V^{*ij} is the measure on the real network. Note that the total number of distinct couples (i, j) and therefore the number of different hypotheses which are tested simultaneously is $N_i(N_i - 1)/2$. Among other proposals for multiple hypotheses testing, the false discovery rate (FDR) [26] permits a control at each step of the verification procedure. The p -values are ordered according to their values from smallest to largest and label by k . The largest \hat{k}

that satisfies

$$p_{value}^{\hat{k}} \leq \frac{\hat{k}\alpha}{N_i(N_i - 1)/2}, \quad (16)$$

defines the effective threshold $p_{th} = \frac{\hat{k}\alpha}{N_i(N_i - 1)/2}$: the hypotheses associated to all p -values smaller than or equal to p_{th} are rejected and are declared as “statistically significant”, i.e. they cannot be explained by the null-model. Once the p -value associated with the couple (i, j) is rejected, in the projected network a binary link is drawn between the two nodes.

APPENDIX B: LIMITS OF THE BIRG AND THE BIPCM_c PROJECTION ON THE PRODUCTS LAYER

The performance of the grand canonical projection algorithm depends on the choice of the null-model, which defines the information of the original bipartite network to be discounted in the link verification process. As already mentioned in the main text, the BiCM imposes the most stringent constraints. For comparison with the BiPCM_p product network, Fig. 8 illustrates the product networks obtained if the BiPCM_c and the BiRG are applied, i.e. if the nodes of the country layer or the total number of edges are fixed, respectively. It is easy to see that the two are topologically very different from Fig. 5: while the BiPCM_p network is highly fragmented, the BiRG and BiPCM_c networks are dominated by the presence of a large connected component, which contains almost all the nodes. The few isolated clusters are composed of (“meat of swine”, “pig fat”) and (“cocoa paste”, “cocoa butter”), and of (“chromium oxides and hydroxides”, “salts of oxometallic or peroxometallic acids”), respectively. These product couples are thus extraordinarily often exported together compared to others. The difference between the models is also shown in Fig. 9. While the BiRG acts as a relatively “coarse” filter, the statistical verification becomes more strict passing from the BiPCM_c to the BiPCM_p and ultimately to the BiCM, for which no links are verified. This observation is substantially due to the fact that the node-specific probability distributions of the V^{ij} -motifs collapse into a single distribution for the BiRG and the BiPCM_c, which turn out to be Binomial and Poisson Binomial [19]. Consequently, the null-models induce a one-to-one mapping of the V^{ij} measurements onto the p -values. Imposing a significance level for hypothesis testing amounts therefore to choosing a threshold value $V_{ij,th}$ and discarding motifs with $V_{ij} < V_{ij,th}$. For the BiRG, $V_{ij,th} \in \{9, 10\}$, whereas for the BiPCM_c $V_{ij,th} \in \{12, 13, 14\}$, depending on the year in the interval 1995 - 2010. As a consequence, only products with $V_{ij} \geq V_{ij,th}$ bear significant similarity. The only difference between the motif validations with BiRG and BiPCM_c is a shift in the p -value threshold. The

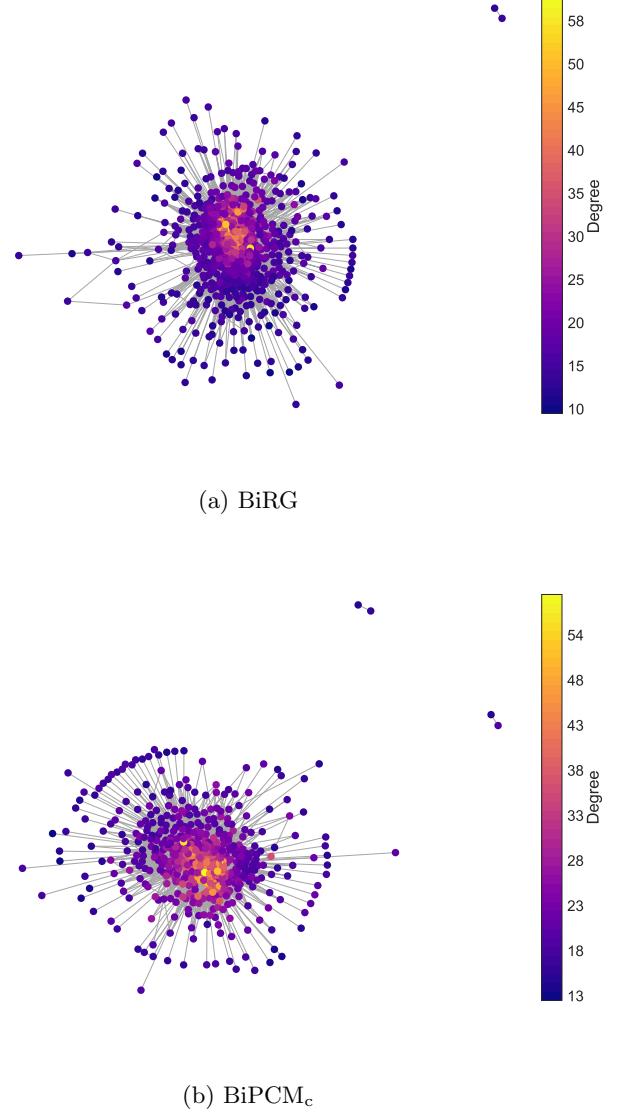
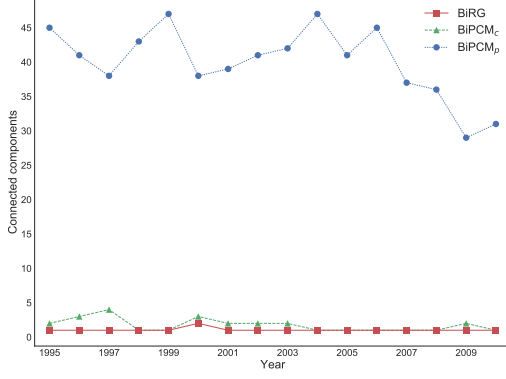
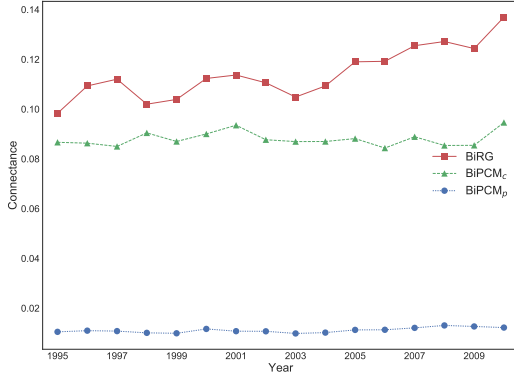


Figure 8: BiRG and BiPCM_c product networks for the year 2000. The networks are dominated by the largest connected components whose cores are composed of high degree nodes. The degree values refer to the original country-product bipartite network.

cores of the projection networks host almost exclusively nodes with degrees in the original bipartite network, as one can confirm by closer inspection of Fig. 8. It is worth pointing out that several edges in the BiRG model have p -values which are smaller than the machine precision $\simeq 2.22 \cdot 10^{-16}$.



(a) Number of connected components in the projected product networks.



(b) Connectance of the projected product networks.

Figure 9: Properties of the product networks spanned by the statistically significant edges according to the respective null-models. The BiPCM_p network is highly fragmented, as shown by the comparatively large number of connected components in (a) and the low connectance, see (b). On the other hand, both BiRG and BiPCM_c are composed of comparatively densely connected clusters. Isolated nodes are ignored in both figures.